Early Prediction of Breast Cancer Therapeutic Response and Evaluation of Residual Disease Using Quantitative DCE-MRI

Alina Tudorica[1], Karen Y Oh[1], Stephen Y-C Chui[1], Nicole Roy[1], Megan L Troxell[1], Yiyi Chen[1], Arpana Naik[1], Ariel Lopez-Chavez[1], Megan L Holtorf[1], Aneela Afzal[1], Mohan Jayatilake[1], Zunqiu Chen[1], Charles S Springer[1], Xin Li[1], and Wei Huang[1]

[1]*Oregon Health & Science University, Portland, OR, United States*

Target Audience: Radiologist, Oncologist, and MRI scientist

Purpose: Neoadjuvant chemotherapy (NACT) is increasingly used before surgery to treat locally advanced breast cancer. Though pathological response is a good indicator of survival, it can be determined only after surgery. Thus, there is a pressing need for minimally invasive imaging methods to provide early prediction of therapeutic response, potentially allowing swift introduction of alternative treatment for non-responding patients. In addition, accurate assessment of residual disease following NACT completion improves surgical decisions of breast conservation *vs.* mastectomy.

Tumor size measurement by breast imaging is the current standard of care for evaluating therapy response. However, changes in tumor size often occur late during treatment (1,2) and may over- or under-estimate residual disease (3). By measuring tumor microvascular properties, quantitative dynamic contrast-enhanced (DCE) MRI has been shown to be effective in early prediction of breast cancer response to NACT (1,4). Taking into account the intercompartmental water exchange kinetics, the Shutter-Speed model (SSM) (5) for DCE-MRI data pharmacokinetic analysis provides a more sensitive measure of tumor vasculature changes compared to the Standard (Tofts) model (SM) (6). Further, the SSM analysis includes an important variable, the mean intracellular water lifetime τ_i, which has been found inversely related to cellular energy metabolism (7). Here we report preliminary results of SSM and SM DCE-MRI evaluations of breast cancer response to therapy.

Methods: Eleven consecutive women with locally advanced breast cancer who underwent NACT consented to research DCE-MRI studies performed at time-point zero (TP_0) - before NACT, at TP_1 - after first NACT cycle, at TP_2 – midpoint of NACT (usually after three NACT cycles), and at TP_3 - after NACT completion. Axial bilateral DCE-MRI images with fat-saturation and full breast coverage were acquired with a 3D gradient echo-based TWIST sequence (8) using a 3T Siemens scanner. DCE-MRI acquisition parameters included 10° flip angle, 2.9/6.2 ms TE/TR, a parallel imaging acceleration factor of two, 30-34 cm FOV, 320x320 matrix size, and 1.4 mm slice thickness. The total acquisition time was ~ 10 min for 32-34 image volume sets with 18-20 s temporal resolution. Gd contrast agent (Prohance®) IV injection (0.1 mmol/kg at 2 mL/s) was carried out following acquisitions of two baseline image volumes. Tumor ROIs were drawn by experienced radiologists who also measured tumor size according to well-established (one dimensional) RECIST (9) guidelines. The ROI and pixel-by-pixel (within the ROI) DCE time-course data were subjected to both the SM and the SSM pharmacokinetic analyses to extract K^{trans}, v_e, k_{ep} (= K^{trans}/v_e), and τ_i (SSM only) parameters. The ΔK^{trans} parameter [= K^{trans}(SSM) - K^{trans}(SM)], which is a measure of the exchange effects on K^{trans} quantification (6,8), was also calculated. The whole tumor mean parameter values were calculated as the weighted (by ROI pixel number) averages of the ROI values from each of the image slices covering the entire tumor.

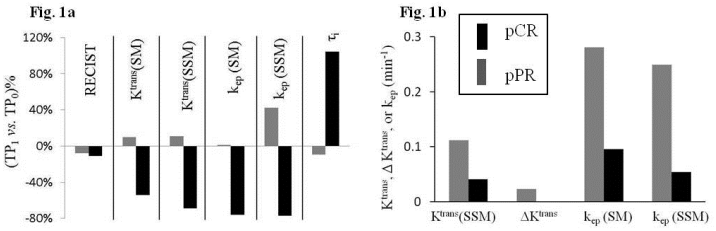

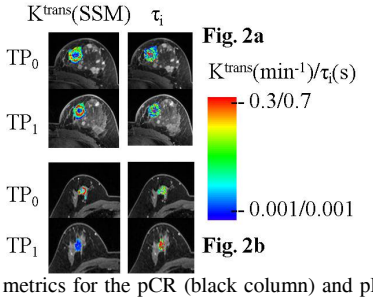

Fig. 2a

Fig. 2b

Pathologic response to NACT and residual cancer burden (RCB) for each patient were determined by pathological analysis of post-therapy surgical specimens and comparison with pre-therapy biopsy specimens using previously published methods (10,11). The pathologic endpoints were correlated with the MRI metrics using the univariate logistic regression (ULR) analysis and the Spearman's correlation (SC) to identify imaging biomarkers for early prediction of response and/or accurate assessment of residual disease following NACT.

Results: Pathological analyses revealed that three patients were pathologic complete responders (pCR) – no cancer cell found in surgical specimens, while the other eight were pathologic partial responders (pPR) – reduced cancer cell density in surgical specimens compared to biopsy specimens. The ULR analysis found that the % changes in tumor mean K^{trans} (SM and SSM), k_{ep} (SM and SSM), and pixel τ_i histogram median after the first NACT cycle (at TP_1 relative to TP_0) were able to completely discriminate the 3 pCRs from the 8 pPRs with the ULR c statistics value = 1, while the TP_1 RECIST % change was a poor predictor of response with c = 0.60. **Fig. 1a** shows a column graph of the mean % changes of these MRI metrics for the pCR (black column) and pPR (gray column) groups. In addition, the absolute values of TP_1 tumor mean K^{trans}(SSM), ΔK^{trans}, and k_{ep} (SM and SSM) (**Fig. 1b**) were also able to completely separate the two groups. The ΔK^{trans} column for the pCR group is invisible in Fig. 1b because its mean value was near zero. **Fig. 2** shows the tumor K^{trans}(SSM) and τ_i maps (in color) of a pPR (2a) and a pCR (2b) at TP_0 and TP_1. Compared to the pPR, the decrease in K^{trans}(SSM) and increase in τ_i from TP_0 to TP_1 were dramatic for the pCR. The RCB can be described in numerical values or ranks (such as I, II, III, *etc.*) with RCB = 0 indicating pCR (10,11). ULR analysis and SC were used to correlate TP_3 (after NACT completion) MRI metrics with RCB ranks and actual values, respectively. The **Table** shows that the TP_3 tumor mean τ_i and K^{trans} (SM and SSM) were good markers of RCB ranks, while the RECIST measure was a fair marker. The SC analysis revealed that τ_i was inversely while K^{trans} and RECIST were positively correlated with RCB. The correlations were statistically significant ($P \leq 0.05$) for τ_i and K^{trans} (SSM).

Table. Correlations of TP_3 MRI Metrics with RCB

MRI Metrics	c (ULR)	SC coeff.	P
τ_i	0.878	-0.62	0.04
K^{trans}(SSM)	0.829	0.60	0.05
K^{trans}(SM)	0.829	0.50	0.11
RECIST	0.732	0.55	0.08

Discussion and Conclusion: Consistent with previous studies (1,4), our preliminary results suggest that changes in tumor microvasculature precede size changes in response to NACT. After only one cycle of NACT, the % changes (relative to baseline) or actual values of quantitative DCE-MRI biomarkers can predict eventual pathologic response to the entire course of NACT, while the RECIST measure of tumor size is not a good predictor of response at this time point or even the midpoint of NACT (results not shown here). Both SM and SSM K^{trans} and k_{ep} parameters are excellent early predictors. However, the changes in the SSM parameters generally offer larger separations of the two response groups (see Fig. 1a) and thus are more sensitive measures of therapeutic response. This is most likely due to the incorporation of the exchange effects in the SSM analysis (5). Furthermore, the SSM method provides an additional biomarker, τ_i, for assessment of response, which cannot be accessed by the SM method. τ_i may add a metabolic dimension (7) in DCE-MRI evaluation of therapy response and its potential is manifested in early prediction of response and accurate assessment of residual disease. In conclusion, this preliminary study demonstrates that quantitative DCE-MRI, particularly the SSM approach, is superior to tumor size measurement for early prediction of breast cancer response to therapy and evaluation of residual disease after therapy. Enrollment of a larger population is planned to validate the initial findings.

Grant Support: NIH: UO1-CA154602, RO1-NS040801.

References: **1.** Marinovich *et al. The Breast* 2012;21:669-677. **2.** Tan *et al. Magn Reson Imaging* 2008;26:26-34. **3.** Partridge *et al. AJR* 2002;179:1193-9. **4.** Ah-See *et al. Clin cancer Res* 2008;14: 6580-9. **5.** Huang *et al. Radiology* 2011;261: 394-403. **6.** Tofts *et al. JMRI* 1999;10:223-32. **7.** Zhang *et al. Biophys J* 2011;101:2833-42. **8.** Tudorica *et al. Magn Reson Imaging* 2012;30:1257-67. **9.** Therasse *et al. J Natl Cancer Inst* 2000;92:205-16. **10.** Symmans *et al. J Clin Oncol* 2007;25:4414-22. **11.** Rajan *et al. Cancer* 2004;100:1365-73.